Ordinary and Transition Regime Diffusion in Random Fiber Structures

Manolis M. Tomadakis and Stratis V. Sotirchos
Dept. of Chemical Engineering, University of Rochester, Rochester, NY 14627

The problem of bulk, transition and Knudsen regime diffusion in structures of freely overlapping fibers of various orientation distributions was numerically investigated, and the interrelation of the resulting effective diffusivities was examined. Fibers were randomly positioned and oriented in $d = 1$, 2, or 3 directions. A Monte Carlo simulation scheme was employed to determine the effective diffusivities from the mean-square displacement of random walkers traveling in the interior of the porous structure. The effective diffusivity was found to depend strongly on the orientational distribution of the fibers, porosity of the fibrous structures, and Knudsen number. The tortuosity factor decreased in general with increasing porosity, approaching at the limit of dilute beds the lower bound derived for each direction of diffusion from variational principles. The simulation results agreed well with experimental values of the bulk tortuosity of fibrous beds from the literature. It was also found that the reciprocal additivity or harmonic average effective diffusivity expression (Bosanquet formula), commonly used to estimate transition regime diffusivities from the values at the ordinary and Knudsen diffusion limits, provides an excellent approximation for the effective diffusivity of fibrous beds, except for that parallel to the fibers of a unidirectional structure.

Introduction

Various technological applications of fibrous porous media were outlined in our previous studies (Tomadakis and Sotirchos, 1991a,b), where fibrous structures were studied with regard to the dependence of their Knudsen diffusivities and structural properties on porosity and extent of fiber overlapping. Fibrous porous media, however, have usually macroporous structure, and as a result, in most applications involving them [chemical vapor infiltration, for instance (Sotirchos, 1991)], diffusion takes place under conditions where the average wall-to-wall distance in the pore space is comparable to or much larger than the mean free path of the diffusing molecules in the fluid phase, even during gaseous diffusion at subambient pressures. Therefore, knowledge of the mass transport behavior of fibrous porous media in the entire diffusion regime is needed in general when mathematical models of processes that involve mass transport in such structures are developed.

The variation of the effective diffusion coefficient of random fiber structures with the porosity in the transition and bulk diffusion regime is numerically studied in detail in this work. We consider fiber structures formed by cylindrical fibers distributed randomly in d ($d = 1$, 2, or 3) directions (d-directional, random fiber structures): with their axes parallel to a line ($d = 1$), parallel to a plane ($d = 2$), or oriented randomly in the three-dimensional space ($d = 3$). Structures with fibers grouped into d ($d = 1$, 2, or 3) bundles of parallel, randomly overlapping fibers, with the bundles arranged in mutually perpendicular directions (d-directional, parallel fiber structures), are not considered in this study, since in our previous study (Tomadakis and Sotirchos, 1991a), it was found that they exhibit transport and structural properties identical to those of the corresponding d-directional, random fiber structures. Our study is based on the use of a molecular simulation procedure, utilizing a combination of the mean-square displacement method with a step-by-step random walk mechanism. The method rests on computing the trajectories of a large number of random walkers introduced randomly in a finite sample (unit cell) of the fiber structure and using them to

Correspondence concerning this article should be addressed to S. V. Sotirchos.

compute the mean-square displacement of the walkers from their initial positions for sufficiently large travel times. The effective diffusivity is then found from the mean-square displacement equation (Einstein, 1926; Kennard, 1938; Chandrasekhar, 1943; Rahman, 1964), appropriately modified to account for the presence of the solid phase.

Analytical and numerical approaches for studying transition and continuum regime flows are reviewed by Bird (1976), who also discusses a dynamic molecular simulation algorithm, in which, in contrast to the method used in our study, the movements and collisions of thousands of molecules are followed simultaneously. However, the computational cost of such an explicit approach is prohibitive, if a relatively large region of the parametric space of the problem (such as large porosity range) is to be investigated. Ordinary regime diffusion can also be simulated by employing random walks based on the first passage time (FPT) probability distribution (Brown, 1956; Siegel and Langer, 1986; Zheng and Chiew, 1988; Torquato and Kim, 1989; Tassopoulos and Rosner, 1992; Melkote and Jensen, 1992). Instead of moving the molecule step-by-step in the porous medium, such random walks advance it to a random point on the surface of a sphere centered at the current position of the walker and tangent to the closest solid surface. The time corresponding to this movement is sampled from the FPT probability distribution or given an average value calculated from the radius of the sphere and the diffusivity in the absence of the porous medium.

FPT-based methods can lead to a significant reduction of the computational time needed to follow the sojourn of a molecule in the interior of a porous medium, but they cannot provide explicit information on the frequency of intermolecular and molecule-wall collisions and the distribution of free paths between like and unlike collisions. Moreover, they cannot be used to study diffusion in the transition regime; even in the ordinary diffusion regime, they must be combined with a discrete step-by-step random walk in order to account for molecule-wall collisions. This necessitates the use of an adjustable computational parameter, the thickness of a boundary layer around the walls of the porous medium that defines the limits of the area where the discrete random walk has to be followed. The minimum value of this parameter that does not introduce any bias in the simulation results has to be determined carefully on the basis of repetitive calculations (Tassopoulos and Rosner, 1992; Melkote and Jensen, 1992). When an adequately large value is assigned to this parameter, FPT-based procedures give results identical to those of a discrete random walk technique.

Past theoretical work on ordinary diffusion in fibrous structures has primarily been focused on the derivation of upper bounds or approximations to the effective diffusivity using variational principles or other analytical methods (Milton, 1981; Tsai and Strieder, 1986; Torquato and Beasley, 1986; Joslin and Stell, 1986a,b). A numerical study on transition and bulk diffusion in fibrous beds was presented by Melkote and Jensen (1992), who employed a random walk procedure based on the concept of the first passage time to compute the effective diffusivity. Melkote and Jensen worked on three-directional fiber structures, but, as we will explain in some more detail later, their results are not representative of random fiber structures and therefore cannot be compared with those predicted in this study.

The results of our computations are used to develop correlations for the dependence of the tortuosity factor for diffusion in the ordinary, transition, and Knudsen diffusion regime for use in mathematical models of processes involving mass transport in porous media of fibrous structure. For the special case of ordinary regime diffusion, the numerically computed diffusivities are compared with a few experimental data found in the literature (Penman, 1940; Currie, 1960; Bateman et al., 1984). Several expressions are examined for prediction of the diffusivity in the transition regime from the values at the two extremes of ordinary and Knudsen diffusion. Particular emphasis is placed on the harmonic average or reciprocal additivity relationship, proposed by Bosanquet (cited by Pollard and Present, 1948) for self-diffusion in cylindrical tubes and later transformed, on the basis of some analytical results, into an equivalent expression for diffusion in porous media of arbitrary structure (Rothfeld, 1963; Spiegler, 1966; Ho and Strieder, 1979, 1980; Tokunanga, 1985). The Bosanquet equation is the most frequently used expression for effective diffusivity determination in the transition regime, and it was among the basic laws that Evans and Watson (1961) applied in the development of their dusty-gas model. Our results show that the reciprocal additivity can be used to obtain an excellent approximation to the effective diffusivity in the transition regime from the two extreme diffusivities, for certain directions of diffusion in the general case of an anisotropic medium, and this is the first time that such a conclusion is presented in the literature.

Method of Construction of the Unit Cell

It is readily seen that the problem of generating a random fiber structure is equivalent to the geometric problem of drawing random lines in space. When performing molecular simulations, however, one has to use a finite unit cell, and thus, the problem is further transformed into that of drawing random chords in a cube (for a cubic unit cell) or any convex body, in general. Coleman (1969) described various mechanisms by which randomness of straight line paths (secants) through convex bodies can arise. He used the term mean free path randomness or μ-randomness to characterize the mechanism that gives rise to a secant distribution that is identical to that obtained when the convex body is introduced into a population of randomly distributed lines. According to this mechanism, a secant is defined by a point on a fixed plane and its direction with respect to the plane. The point is obtained randomly from a uniform distribution, and the direction independently, on the basis of a probability measure that is reflection invariant with respect to the surface of the convex body. This measure, of course, is bounded so that only the class of points and directions which define a secant of the body is considered.

The μ-randomness mechanism was employed for the construction of the fibrous structures used in this study. A polar coordinate system, located at the trace of each line on the fixed plane was used to determine the direction cosines of the line. The azimuthal angle was sampled from a uniform distribution (between 0 and 2π), and the cosine law was used for determining the polar angle, that is, the square of its cosine was sampled from a uniform distribution (between 0 and 1). For two-directional structures, the azimuthal angle was assigned a fixed value for all lines, while for one-directional structures, all lines were given the same direction cosines. A detailed

description of the construction procedure is given elsewhere (Tomadakis, 1993). It should be pointed out that random fiber structures that obey the μ-randomness mechanism can also be constructed by choosing random points on the boundary of the unit cell and using them to draw random secants according to the cosine law (Burganos and Sotirchos, 1989a). By treating the lines as axes of fibers of radius r, a finite sample of a structure of freely overlapping, randomly positioned in space fibers is obtained. The porosity, ϵ, surface area, S, and mean intercept length, $\bar{d}$—mean length of the segments of a randomly drawn line that lie in the void space—of such a structure are given by (Tomadakis and Sotirchos, 1991a):

$$\epsilon = \exp(-\pi l r^2); \quad Sr = -2\epsilon \ln\epsilon; \quad \bar{d} = 4\epsilon/S = -2r/\ln\epsilon \qquad (1a\text{-}c)$$

with l being the density of fiber axes, that is, the length of lines (fiber axes) per unit volume of porous medium.

Melkote and Jensen (1992) used an interior radiator mechanism [I-randomness in the terminology of Coleman (1969)] to generate finite samples of the fiber structures they used in their work. The same construction scheme was also employed in their study of Knudsen diffusion in fibrous beds (Melkote and Jensen, 1989). According to this scheme, random secants are generated in the convex body (unit cell) by choosing random points in the interior of the porous medium and drawing lines passing through these points in uniformly random directions. The structures generated through the I-randomness mechanism differ fundamentally from those obtained from the μ-randomness mechanism. For instance, the mean length of I-random secants in a cube of unit side is 0.896, whereas the corresponding value for μ-random secants is 0.667 (Coleman, 1969). Moreover, the density of I-random secants (length of lines per unit volume) varies from one point in the convex body to another, and as a result, the porous medium obtained by treating the secants as fiber axes has spatially varying porosity and surface area.

Mean-Square Displacement Method

Effective diffusivities in the Knudsen, transition and bulk diffusion regimes can be computed from the mean-square displacement, $\langle \xi^2 \rangle$, of a large number of identical molecules introduced randomly in the unit cell for adequately large values of travel time, τ. The equation that relates the effective diffusivity, the travel time, and $\langle \xi^2 \rangle$ is derived from the expression for the displacement probability of the molecules in the medium, which is in turn derived by solving the diffusion equation (Fick's second law) for an instantaneous source of molecules at position zero. The resulting expressions (Einstein, 1926; Kennard, 1938; Chandrasekhar, 1943; Rahman, 1964) are:

$$D_e = \frac{\langle \xi^2 \rangle}{6\tau}; \quad D_e(x, y, \text{ or } z) = \frac{\langle \xi^2_{x,y, \text{ or } z} \rangle}{2\tau} \qquad (2a,b)$$

$\langle \xi^2 \rangle$ is used to obtain the orientationally averaged effective diffusivity, D_e (1/3 of the trace of the effective diffusivity tensor), while the mean-square component of the displacement in the x, y, or z direction, $\langle \xi^2_{x,y, \text{ or } z} \rangle$, gives the effective diffusivities associated with diffusion in these directions. Chandrasekhar (1943) derived the diffusion equations from an expression for the probability of displacement of a random walker, thus providing a direct interpretation of the problem of random flights in terms of a diffusion coefficient.

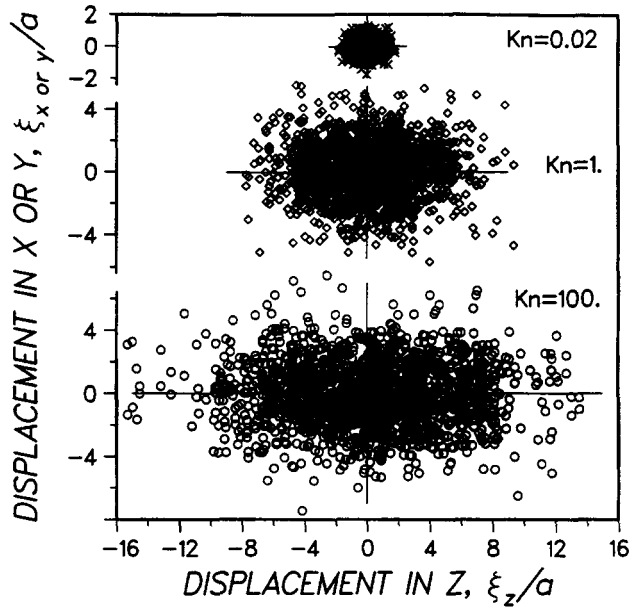

Figure 1. Molecular displacements in all diffusion regimes in a unidirectional fiber structure of 70% porosity with fibers aligned parallel to the z direction.

a is the unit cell size.

Figure 1 shows the positions on the xz and yz planes of the displacements of 800 molecules that have all traveled exactly the same distance, namely 200 cell sides or 10,256 fiber radii, in the three regimes of diffusion in a unidirectional fiber structure of porosity $\epsilon = 0.70$. Since there are two traces for each molecule, on the xz and yz planes, 1,600 points are plotted in each of the three cases shown in Figure 1. The Knudsen number, Kn, defined as the ratio of the continuum mean free path of the molecules, $\bar{\lambda}$, to the mean intercept length ($\bar{d}$) is used to parameterize the diffusion process in the fiber structure. For $Kn = 0.02$ diffusion practically occurs in the ordinary diffusion regime, while for $Kn = 100$ molecule-molecule collisions are rare, and Knudsen diffusion is the dominant mode of diffusion. It is clear from Figure 1 that the effective diffusivity increases as we move from the bulk to the Knudsen diffusion regime. Another interesting observation is that the diffusivity parallel to the fibers—the fibers are aligned parallel to the z direction—is much larger than that in the x or y direction, but the difference between them appears to decrease as diffusion moves closer to the bulk regime.

The histogram of the distribution of molecular displacements in the y direction for the bulk diffusion case of Figure 1 ($Kn = 0.02$) is shown in Figure 2, and qualitatively similar plots are obtained for other directions and regimes of diffusion. The distribution of Figure 2 yields mean displacement almost equal to zero, as it is expected theoretically, and mean-square displacement equal to 0.179. (Note that since this value of mean-square displacement is based only on molecules that fall in the void space, it has to be multiplied by the porosity before it is used in Eq. 2b to compute the effective diffusivity.) The

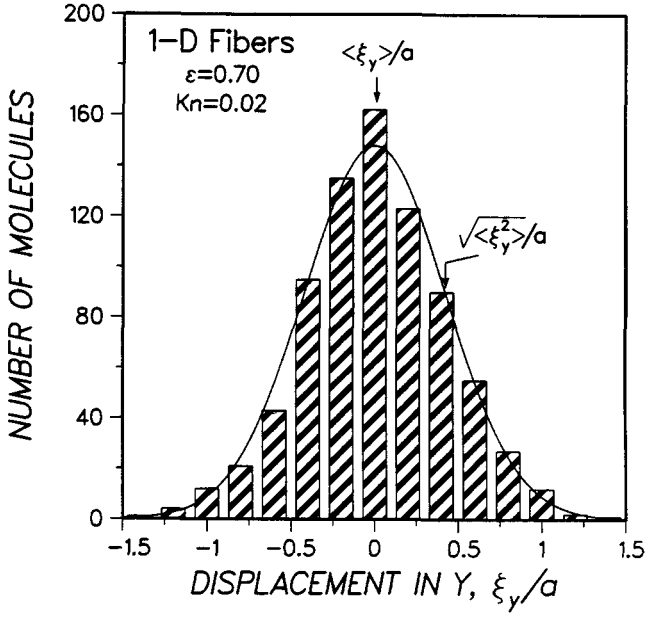

Figure 2. Computed histogram of distribution of molecular displacements for the bulk diffusion case of Figure 1 ($Kn = 0.02$) vs. Gaussian distribution density (solid curve) obtained from the solution of the diffusion equation.

solid curve of Figure 2 is the Gaussian distribution of displacements with variance equal to $\sqrt{\langle \xi_y^2 \rangle}/a$, which is predicted from the solution of the diffusion equation. Very good agreement is seen to exist between the numerically computed distribution and the one predicted from the theory.

Figure 3 shows the evolution of the mean-square displacement with the travel distance, for 800 molecules traveling in a three-directional fiber structure of 60% porosity. For very small travel distance, s, the molecules do not have a chance

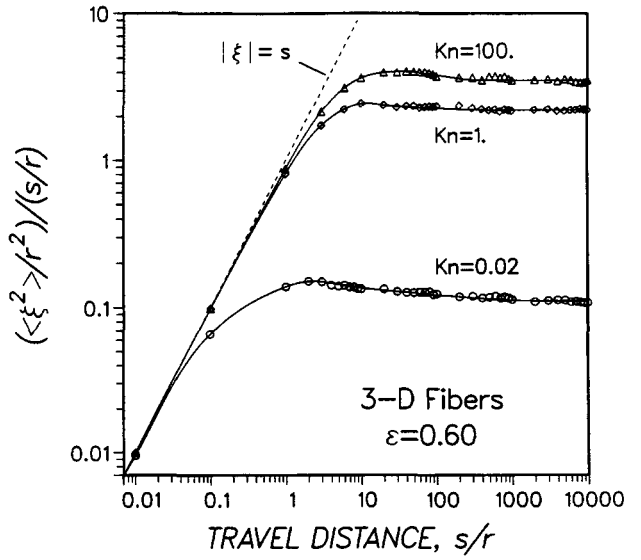

Figure 3. Variation of the (mean-square displacement/travel distance) ratio with the travel distance in a 3-d fiber structure for various Knudsen numbers.

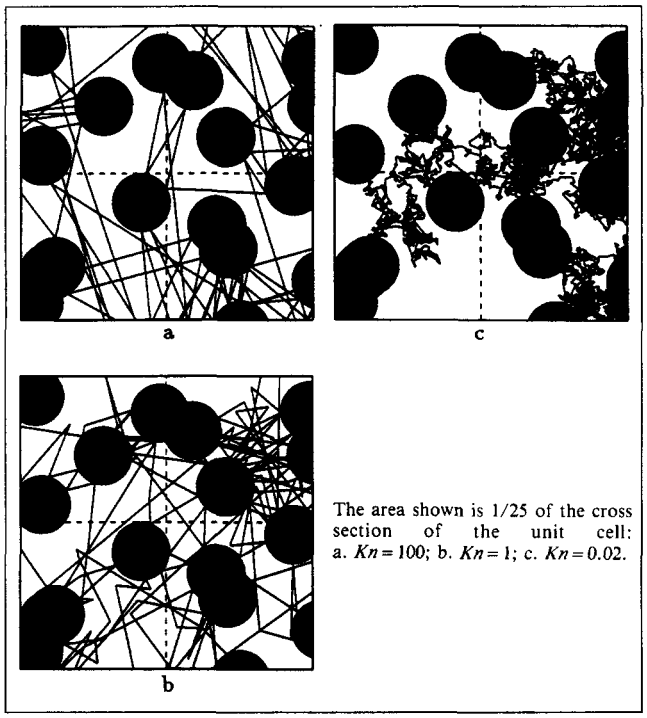

Figure 4. Projections of molecular trajectories on a cross section of the unidirectional fiber structure used to obtain Figures 1 and 2.

to feel the presence of other molecules and walls, and as a result, the magnitude of their displacement, $|\xi|$, is equal to s. This is not the case for large travel distances, where other molecules and fiber walls obstruct the movement of molecules and eventually force $\langle \xi^2 \rangle / s$ to approach a certain value, which depends on the diffusion regime (the Knudsen number) and the porosity. Equations 16 and 18 will show that for the structure used for the computations of Figure 3, the dimensionless travel distance, s/r, is approximately equal to four times the average number of the molecule's collisions with the solid walls.

Step-by-Step Random Walk Procedure

Molecular trajectories for the three cases of Figure 1 are shown in Figure 4. Figure 4a presents part of the trajectory of a molecule diffusing in a unidirectional fiber structure in the Knudsen diffusion regime. What is actually shown there is the projection of the trajectory on a plane perpendicular to the fibers and, more specifically, on an area equal to 1/25th of a face of the unit cell. Figure 4b presents the equivalent projection of a transition regime trajectory, in which the numbers of molecule-wall and intermolecular collisions are of comparable magnitudes. Finally, the corresponding picture for the bulk diffusion regime is given in Figure 4c, where intermolecular collisions are seen to dominate. The molecular trajectories of Figure 4 are typical of the molecular trajectories used to obtain all results in this study. Next, we will briefly describe the discrete random walk procedure employed for the computations.

Trajectory computations begin with generating a random position from three independent uniform distributions in the

unit cubic cell. If the point lies in the solid (in the fibers), a new position is generated; if it lies in the void space, it becomes the starting position of a molecular trajectory. Random direction cosines are consequently assigned to the random walker, and the position of the next potential intermolecular collision is located. This is done by sampling a molecular free path, λ, from an exponential distribution (Jeans, 1925; Loeb, 1934; Kennard, 1938). [Jeans (1925) states that the exponential distribution of continuum free paths is strictly valid for gas molecules moving with constant velocity. He presents a more accurate expression based on the Maxwellian distribution of velocities; however, when he evaluates numerically the involved integrals, he finds insignificant differences from the exponential law (<1%). Loeb (1934) refers to experimental verifications of the exponential distribution law for the free path of silver atoms diffusing in air or nitrogen.] Next, it has to be checked whether the random walker can indeed travel a distance λ on the predicted direction without interference from a fiber or a boundary of the cell. As long as no such interference is encountered, the above procedure is repeatedly applied to generate a sequence of intermolecular collisions.

When one or more fibers are found to lie within the chosen free path, the shortest distance from the point of last collision to the fibers is used to locate the point of molecule-wall collision. A new set of direction cosines is then assigned to the random walker to account for reflection from the fiber wall. Diffuse reflection is assumed to occur since specular reflection of gas molecules on a solid surface is highly unrealistic, while diffuse reflection has been experimentally verified for engineering surfaces in contact with gases (Carman, 1956; Bird, 1976). Having determined the direction of the reflection path, one faces the problem of assigning a free path to the molecule reflected from the surface. It is assumed that the path distribution of the reflected molecules is the same as that of the molecules reaching the surface. If $P_\lambda(\lambda)$ is the free path distribution density of the molecules in the gas phase, it can be shown that the distribution of the paths of the molecules from the point of their last collision to a surface is given by $\int_\lambda^\infty P_\lambda(\lambda')d\lambda'/\bar{\lambda}$, with $\bar{\lambda}$ being the mean free path. For constant free path, $P_\lambda(\lambda)=\delta(\lambda-\bar{\lambda})$, this expression gives a uniform distribution (between 0 and $\bar{\lambda}$), while for an exponential $P_\lambda(\lambda)$ (the form used in our simulations), it predicts that the distribution of molecular paths from the gas phase to the surface is identical to $P_\lambda(\lambda)$. The latter result is equivalent to the well-known result in the kinetic theory of gases that the average free path of molecules crossing an imaginary stationary plane is equal to $2\bar{\lambda}$ (Goodman and Wachman, 1976).

When a random walker reaches a boundary of the unit cell, it is reintroduced into the cell by being specularly reflected on the boundary. Employing this kind of boundary conditions is equivalent to considering the infinite porous medium as an assemblage of identical cubic unit cells of side a, arranged in such a way that any two neighboring cells are mirror images of each other with respect to their common face. Our past studies (Tomadakis and Sotirchos, 1991a) showed that this boundary condition does not introduce any bias in the computations.

Computation of Molecular Trajectories

The straightforward application of the step-by-step random walk algorithm requires large amounts of computational time, which for fixed computer resources may limit drastically the parameter space that can be investigated. We will describe in this section a few modifications of the step-by-step random walk algorithm that can lead to dramatic reduction of the time needed to compute molecular trajectories.

Before the computation of molecular trajectories starts, the unit cell is discretized by dividing it into K^3 small cubes, and K^3 lists of the fibers that intersect these cubes (one list for each cube) are generated. $K=10$ was used for all the results reported in this study. Cross sections of four neighboring small cubes for a one-directional fiber structure are shown in Figure 4. Discretization of the unit cell leads to considerable reduction—by almost two orders of magnitude for $K=10$—of the number of fibers that have to be checked for interference with each molecular path. Moreover, it permits a more accurate estimation of the porosity of the fibrous structures by allowing the use of a very high number of tracing points at a fraction of the total computational cost. For instance, it was found that random introduction of 5×10^6 points in the unit cell yielded fourth decimal point accuracy in ϵ. Verlet (1967) and Melkote and Jensen (1992) employed an analogous computer time-saving scheme by generating closest-particle lists during the molecular travel. In their study of diffusion in particle deposits, Tassopoulos and Rosner (1992) applied a scheme resembling the one employed in this study, but with the small cube size being of the order of particle size.

The decision to use $K=10$ in our simulations was based on the results of an investigation of the dependence of the computational time on K. Some of the results are shown in Figure 5, which presents dimensionless computational time vs. K curves for Knudsen diffusion in three-directional beds for various porosities, ϵ, and fiber densities, N_f (number of fibers per unit cell). The computational time was rendered dimensionless by dividing it with the time needed by the molecules to cover the

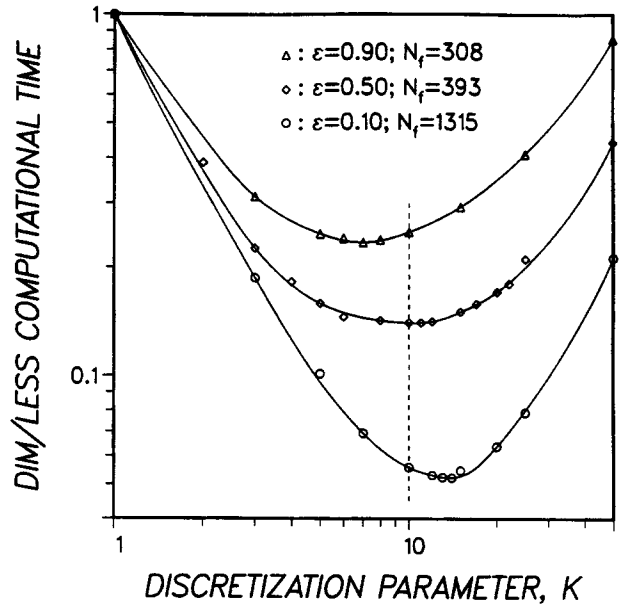

Figure 5. Variation of the computational time with the ratio of unit cell side to small cube side (K) in the domain discretization procedure.

same travel distance in a nondiscretized domain ($K=1$). The results of Figure 5 show that the effect of domain discretization on the computational time decreases with increasing porosity, but this is chiefly due to decreasing number of fibers in the same direction. The optimum value of K increases with increasing fiber density and decreasing porosity, but, as shown in Figure 5, $K=10$ yields computational times very close to the optimum value for all porosities. Similar conclusions were reached for fiber structures of other directionalities. For the three cases shown in Figure 5, the ratio of discretization cell size to fiber size varies between 1.5 and 5.5 at the minimum computational time. This is an indication that the fiber size alone cannot serve as a guide for determining the optimum size of discretization cell.

Further reduction of the computer time requirements of the algorithm is achieved by discretizing the molecular path. Specifically, the path λ, after it is sampled from the exponential free path distribution, is cut into pieces of length equal to one small cube side or less, and the molecule is advanced sequentially until it either completes the sampled path or is obstructed by a fiber. The molecular path can also be discretized by advancing the molecule along the chosen path sequentially from one small cube to its neighbor until collision with the wall or completion of the path is encountered. The effect of path discretization on the computational time becomes stronger as diffusion moves toward the Knudsen regime and longer, relative to the mean intercept length ($\bar{d}$) of the porous medium, free paths for continuum diffusion are encountered.

The bulk diffusion regime is by far the most exacting with respect to computational cost, because, for satisfactory sampling of the pore space, each trajectory must include a large number of molecular paths, each of which has to be checked for interference with the fibers and boundaries of the cell. The computation of molecular trajectories in the bulk diffusion regime can be accelerated considerably by using the following scheme, previously applied by Tassopoulos and Rosner (1992), which exploits the basic idea of FPT-based random walks: at the start of a molecule's travel in the ordinary regime, a sphere centered at the starting position and tangent of the closest fiber surface is constructed. Since the molecule can reach the surface of this sphere for the first time only through intermolecular collisions, there is no need to check for collisions with the fiber walls as long as the molecule moves within the limits of the spherical domain. The spherical inclusion becomes useless when the molecule exits its boundaries. A new tangent sphere is constructed at the point of the first intermolecular collision after the molecule crosses the boundaries of the old inclusion for the first time. The spherical inclusion technique can lead to dramatic reduction of the time needed to compute molecular trajectories in the bulk diffusion regime, but for successful application of the overall algorithm, it must be coordinated carefully with the domain and path discretization schemes and the application of specular boundary conditions.

Information on the displacements ($\xi_{x,y,\text{or}\,z}$ and ξ) of each molecule from its starting position is acquired for several values of travel time (τ) along the same trajectory. Using this information, it is possible to study the variation of the slope of the mean-square displacement vs. τ curve with the travel time, and this way, determine whether the molecules have been given enough time to sample the pore space. Moreover, having mean-square displacement data for several values of travel time makes it possible to obtain more accurate results by using the average of all mean-square displacement vs. τ slopes that correspond to times larger than the minimum time needed to sample the pore space to compute the effective diffusivity (see Figure 3).

Most of the simulation results reported in this study were obtained using 1,600 molecules. We made this choice on the basis of an investigation of the dependence of the accuracy of the simulation results on the number of random walkers (Tomadakis, 1992). The minimum number of molecule-wall collisions required for an adequate sampling of the porous structure by a random walker was found to be practically independent of the diffusion regime, but strongly related to the porosity of the structure. A few hundred of such collisions were enough at high ϵ, but a number of the order of 10^5 was needed in the vicinity of the percolation threshold of the porous structures. In terms of the total number of discrete steps, that is, including intermolecular collisions, the requirements are of the same order for $Kn \geq 1$, but significantly higher for small Knudsen numbers because, as we will see later, the ratio of the numbers of molecule-wall and molecule-molecule collisions is equal to the Knudsen number. These observations are in agreement with those made by other researchers. For instance, Schwartz and Banavar (1989) reported that up to 300,000 steps were required in low-porosity granular samples in the bulk diffusion regime, while Tassopoulos and Rosner (1992) reported a value of 400,000 discrete steps for their simulations in the bulk diffusion regime at intermediate porosity values.

Effective Diffusivities and Tortuosities

The orientationally averaged effective diffusivity and the directional effective diffusivities are used to compute tortuosity factors η and $\eta_{(x,y,\text{or}\,z)}$, respectively, using the equations

$$D_e=\frac{\epsilon}{\eta}D_p;\quad D_{e(x,y,\text{or}\,z)}=\frac{\epsilon}{\eta_{(x,y,\text{or}\,z)}}D_p \tag{3a,b}$$

The reference diffusivity is chosen as the self-diffusion coefficient, D_p, of the diffusing species in a cylindrical pore of diameter equal to the average pore size of the fibrous structure ($\bar{d}$) under the same pressure and temperature (the same continuum mean free path $\bar{\lambda}$) as in the porous medium. D_p is known to follow closely the harmonic average equation proposed by Bosanquet (Pollard and Present, 1948):

$$\frac{1}{D_p}=\frac{1}{D^b}+\frac{1}{D^K} \tag{4}$$

D^b is the bulk self-diffusion coefficient, which for a no-memory random walk is given by $D^b=1/3\bar{v}\bar{\lambda}$, and D^K is the Knudsen diffusivity in a pore of diameter $\bar{d}$: $D^K=1/3\bar{v}\bar{d}$. Introducing the expressions for D^b and D^K in Eq. 4 and using the definition of the Knudsen number ($Kn=\bar{\lambda}/\bar{d}$), Eq. 4 becomes:

$$D_p=\frac{D^b}{1+Kn}=\frac{D^K}{1+\dfrac{1}{Kn}} \tag{5}$$

It is obvious from Eq. 5 that the reference diffusivity, D_p, becomes equal to D^b in the bulk diffusion regime ($Kn \ll 1$) and to D^K in the Knudsen regime ($Kn \gg 1$).

Equation 5 can also be written in the form:

$$D_p = \frac{1}{3}\bar{v}\left(\frac{\bar{\lambda}\bar{d}}{\bar{\lambda}+\bar{d}}\right) = \frac{1}{3}\bar{v}\bar{l} \tag{6}$$

with

$$\frac{1}{\bar{l}} = \frac{1}{\bar{\lambda}} + \frac{1}{\bar{d}} \tag{7}$$

$\bar{l}$, as expressed in Eq. 7, was shown by Bosanquet (Pollard and Present, 1948) to be the average length of molecular steps between successive collisions of any kind for a gas diffusing in a cylindrical tube. As we will see later in this study, this is true for any porous medium, and therefore, the mean path computed from Eq. 7 turns out to be identical to that obtained from the simulation results. It follows from Eq. 6 that the reference diffusivity D_p can physically be interpreted either as the bulk self-diffusion coefficient in a gas of continuum mean free path equal to the actual mean free path of the gas in the porous medium ($\bar{l}$) or as the Knudsen diffusivity of the gas in a cylindrical pore of diameter equal to $\bar{l}$.

Bosanquet's relation for the reciprocal additivity of self-diffusion coefficients is frequently used in applications to obtain estimates of the effective diffusivity in the transition regime by using the effective bulk and Knudsen diffusivities in the place of the single pore values, that is, by writing:

$$\frac{1}{D_{ej}} = \frac{1}{D_{ej}^b} + \frac{1}{D_{ej}^K} \tag{8}$$

with j denoting x, y, or z for the directional diffusivities or nothing for the orientationally averaged diffusivity. Using the definition of the tortuosity factor (Eq. 3) and Eq. 4, Eq. 8 yields the following relation for the transition, Knudsen, and bulk tortuosities:

$$\eta_j = \frac{\eta_j^b + \eta_j^K Kn}{1+Kn} \tag{9}$$

The results of our simulations will be used to test the validity of Eqs. 8 and 9 for diffusion in fibrous beds.

For diffusion in the molecular diffusion regime, where the mean free path is much smaller than the average distance between pore walls, analytical estimates of the effective diffusion coefficients are available in the literature for regular arrays of unidirectional fibers. These results can, therefore, be used to validate the algorithm used for studying gaseous self-diffusion in the transition and bulk regime. Figure 6 compares estimates of the tortuosity factor for bulk diffusion perpendicularly to a regular square array of fibers obtained using our algorithm for bulk and transition regime diffusion with analytical results presented by Perrins et al. (1979). Our simulation estimates are in excellent agreement with the theoretical predictions even though only 200 molecules were used to obtain the mean-square displacements on which the computation of the tortuosity factors of Figure 6 was based.

Variation of the Tortuosity with the Knudsen Number

The variation of the tortuosity factor, η, with the Knudsen number, Kn, for a three-directional random fiber structure is presented in Figure 7. Results for the highly anisotropic one-directional fiber structure are reported in Figure 8. For the results in Figures 7 and 8, 415 and 322 fibers were used, respectively, while for those in other figures, the number of fibers varied between 304 and 1,315 depending on the porosity of the fiber structure. The results of Figures 7 and 8 suggest that the limits of the transition regime extend from about $Kn = 0.02$ to $Kn = 50$, in good agreement with the values reported by Tassopoulos and Rosner (1992) for diffusion in anisotropic

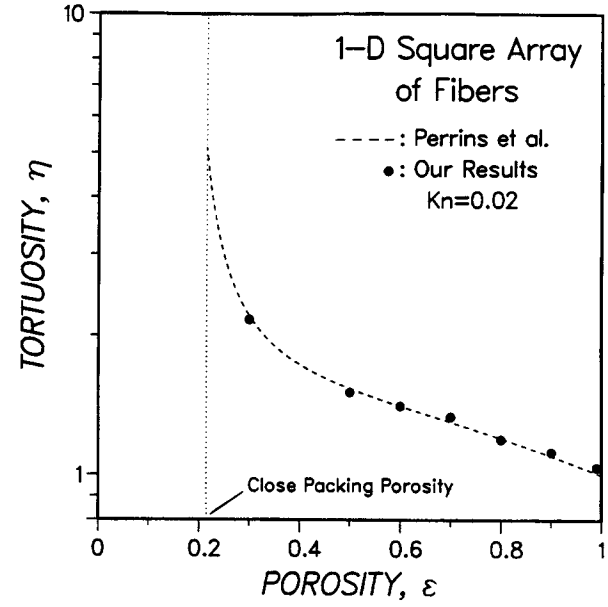

Figure 6. Computed bulk tortuosity factor (distinct data points) vs. theoretically expected value (dashed curve) for diffusion perpendicularly to the fibers of a regular square array.

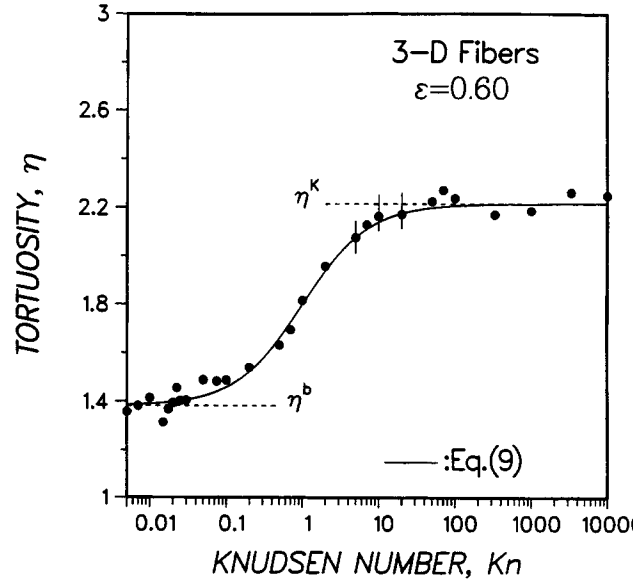

Figure 7. Variation of the tortuosity factor with the Knudsen number in the 3-d fiber structure for $\epsilon = 0.60$.

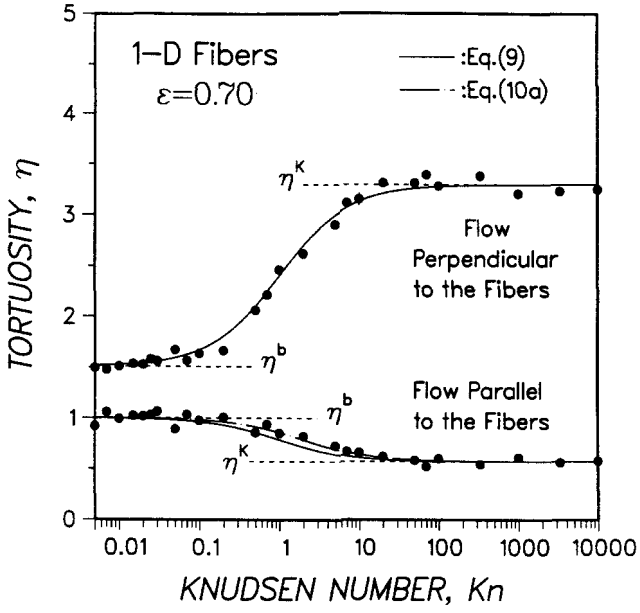

Figure 8. Variation of the tortuosity factors of the unidirectional fiber structure with the Knudsen number for $\epsilon = 0.70$.

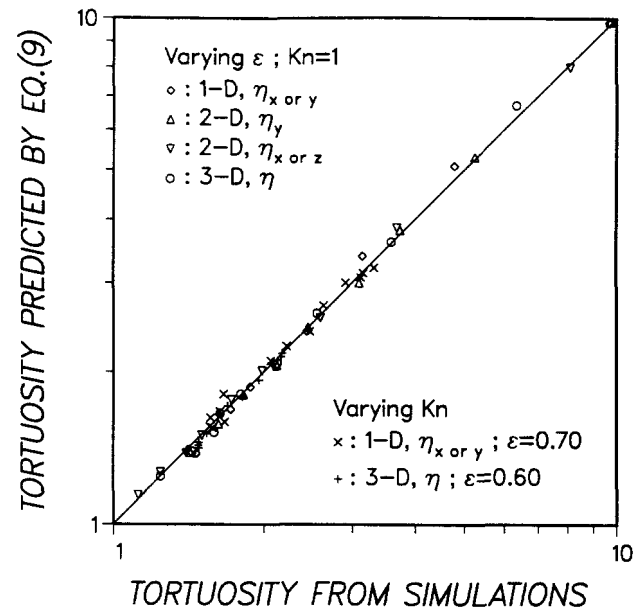

Figure 9. Computed values of the transition regime tortuosity vs. those predicted by Eq. 9 using bulk and Knudsen tortuosities.

particulate deposits (0.01 to 50). In view of this result, the tortuosity factors for bulk and Knudsen diffusion (dashed lines) were determined as the average of all tortuosity factors for $Kn \leq 0.02$ and $Kn \geq 50$, respectively. Error bars are given for three values of Knudsen number in Figure 7 and $Kn = 10$ in Figure 8. Each bar gives the range of values covered by ten different estimates of the tortuosity factor, each estimate obtained using a set of about 800 molecules. With the exception of the points where error bars are shown, all other data plotted in Figure 7 and 8 represent the results of single runs of 800 molecules each. The standard deviation of each set of ten estimates was found to lie in the range of 2.2-2.5% of the average value. Similar was the standard deviation of the bulk and Knudsen tortuosity estimates at different Knudsen numbers. For instance, the eight values of bulk tortuosity in Figure 7 (for $Kn \leq 0.025$) have a standard deviation of 3.1%.

The solid curves in Figures 7 and 8 give the tortuosity predicted by Eq. 9 using the numerically determined values of η^K and η^b. Very good agreement is seen to exist between the result from Eq. 9 and the numerically estimated tortuosity for diffusion in isotropic three-directional structures (Figure 7) and perpendicularly to unidirectional fibers (Figure 8). This is also the case for diffusion in two-directional fibrous structures, both for the directional tortuosities and the orientationally averaged value. Figure 9 compares the directional tortuosities obtained from our simulation data for transition regime diffusion along the principal axes of diffusion, except for diffusion parallel to unidirectional fibers, for various combinations of porosity and Knudsen number with the tortuosities predicted from the Bosanquet equation (Eq. 9). Analysis of the data of Figure 9 indicated that the absolute value of the relative error between the exact (from simulations) and predicted (from Eq. 9) tortuosities, $|(\eta_j)_{\text{exact}} - (\eta_j)_{\text{Eq. 9}}|/(\eta_j)_{\text{exact}}$, had an average value of 2.4% and 2.1% standard deviation, which showed no dependence on porosity, Knudsen number, or fiber directionality. The average ratio of $(\eta_j)_{\text{Eq. 9}}$ to $(\eta_j)_{\text{exact}}$ was found to be equal to 0.9996, indicating the absence of any systematic overprediction or underprediction of the transition regime tortuosity by Eq. 9.

Figure 8 shows that for diffusion parallel to unidirectional fibers, the reciprocal additivity expression systematically underpredicts the tortuosity factor (Eq. 9) and, hence, overpredicts the effective diffusivity (Eq. 8). Specifically, Eq. 9 underpredicted the tortuosity parallel to the fibers by as much as 20% in the vicinity of $Kn = 1$. The average value of the relative error between the exact tortuosity (the result obtained from simulations) and the value found from Eq. 9 for all data points obtained in this study for this configuration of diffusional flow was 8.5% with 4.3% standard deviation. The analysis of the results for diffusion parallel to the fibers (in the z direction) showed that the dependence of the transition regime tortuosity on the Knudsen number can be described by Eq. 10a or, equivalently, 10b in terms of effective diffusivities:

$$\eta_z = \frac{\eta_z^b + \eta_z^K(\gamma Kn)}{1+\gamma Kn}; \quad \frac{1}{D_{ez}} = \left(\frac{1}{D_{ez}^b} + \frac{1}{D_{ez}^K/\gamma}\right)\left(\frac{1+Kn}{1+\gamma Kn}\right) \qquad (10a,b)$$

Linear regression on the data using Eq. 10a $[(\eta_z - \eta_z^b)/(\eta_z^K - \eta_z)$ vs. $Kn]$ gave $\gamma = 0.62$ with 96% correlation coefficient, and this value was used to plot the chain-dotted line in Figure 8.

The fact that the Bosanquet formula (Eq. 8) yields excellent approximations for the effective diffusivities of bi- and tridirectional fiber structures has very important consequences for applications, since it implies that, given the porosity and internal surface area of the porous medium, only the bulk and Knudsen tortuosity factors are needed to determine the effective diffusivity in the transition regime. In view of Eq. 10b, this claim can also be made for unidirectional fiber structures. To the best of our knowledge, this is the first time that the validity of the Bosanquet relationship has been demonstrated

for a pore structure other than a single pore by independent estimation of the bulk, Knudsen, and transition regime diffusivities. The validity of Eq. 8 suggests that correlations whose predictions deviate significantly from those of the Bosanquet formula are inappropriate for estimating transition regime tortuosities in fibrous beds. For example, Wheeler (1955) proposed to estimate the transition regime diffusivity in a single pore from the formula $D_p = D^b(1 - e^{-D^K/D^b})$, which in terms of effective diffusivities becomes $D_{ej} = D^b_{ej}(1 - e^{-D^K_{ej}/D^b_{ej}})$. Using this expression and Eq. 8, we find that the ratio of the diffusivity predicted by Wheeler's expression to the harmonic average diffusivity is equal to $(1+f)(1-e^{-1/f})$ with $f = Kn(\eta^K/\eta^b)$. This ratio is always greater than unity, approaching unity at the limits of bulk and Knudsen diffusion and reaching a maximum of 1.30 at $f = 0.56$, that is, around $Kn = 1$ for diffusion in fibrous structures.

Variation of the Tortuosity with the Porosity

The tortuosity factor in all three regimes of diffusion is plotted in Figure 10 as a function of the porosity for the isotropic three-directional random fiber structure. Analogous results are shown in Figures 11 and 12 for the two-directional fiber structure, perpendicularly to the fibers and parallel to the plane defined by their directions, respectively, and in Figure 13 for the highly anisotropic unidirectional fibers. The values of the bulk tortuosity factor, η^b, were obtained for $Kn = 0.02$, while those of the Knudsen tortuosity factor, η^K, for $Kn = 100$. The transition regime curve was generated for equal continuum mean free path and mean intercept length: $Kn = 1$. A different fiber realization was used for each porosity level in Figures 10, 11 and 12 and 13. It should be pointed out that at a given porosity, the effect of realization on the simulation results and, as a result, the scattering in the data decreases from the Knudsen to the bulk diffusion regime. In agreement with the results presented in our past study on Knudsen diffusion (Tomadakis and Sotirchos, 1991a), the results for two-directional

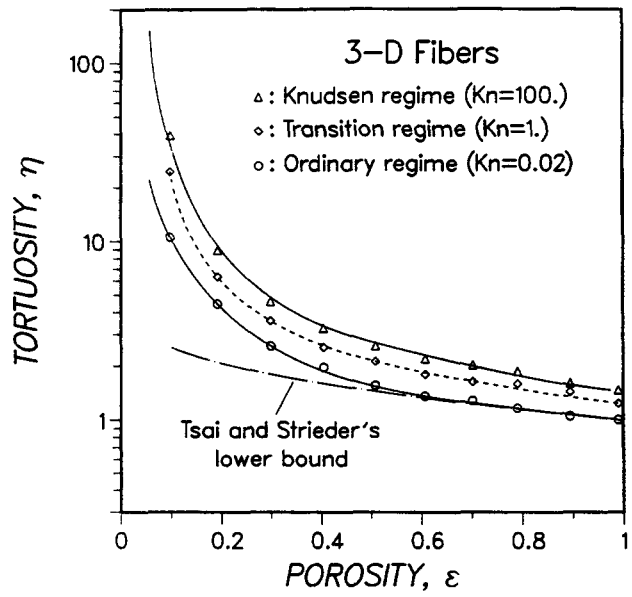

Figure 10. Variation of the tortuosity factor with the porosity for diffusion in 3-d fiber structures.

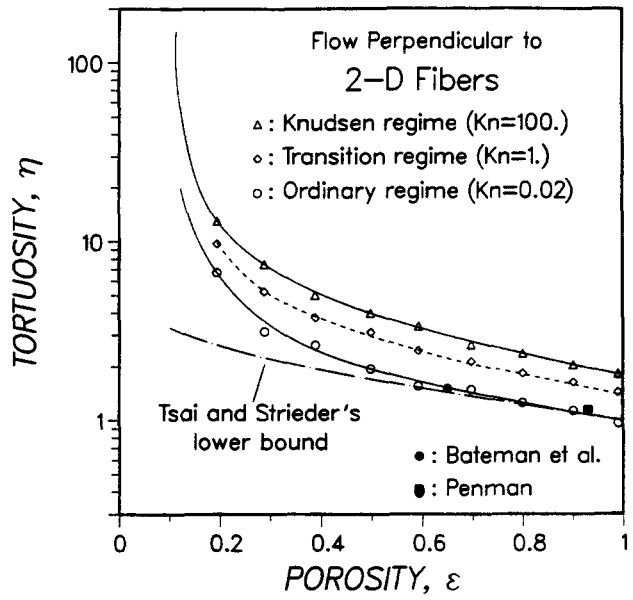

Figure 11. Variation of the tortuosity factor with the porosity for diffusion in bidirectional fiber structures, perpendicular to the plane defined by fiber directions.

fiber structures were more sensitive toward the realization used for diffusion perpendicularly to the fibers.

The results of Figures 10–12 show, in agreement with those of Figures 7 and 8, that the tortuosity factor of two- and three-directional fibrous beds increases from the bulk to the Knudsen diffusion regime. This is also the case for diffusion perpendicularly to unidirectional fibers (Figure 13). For diffusion parallel to such fibers, the tortuosity factor for bulk diffusion is unity at all porosities, while the Knudsen tortuosity is also

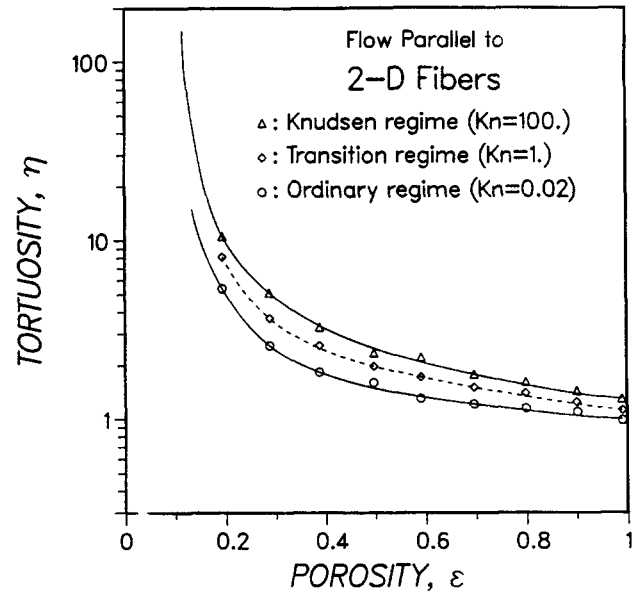

Figure 12. Variation of the tortuosity factor with the porosity for diffusion in bidirectional fiber structures, parallel to the plane defined by fiber directions.

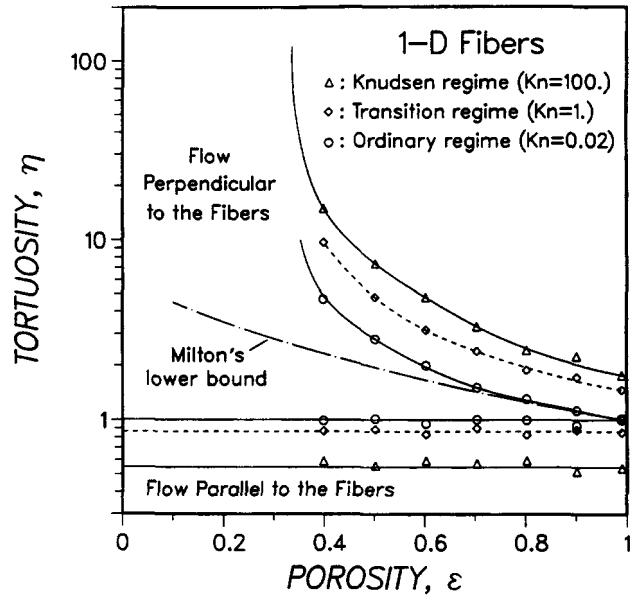

Figure 13. Variation of the tortuosity factor with the porosity for diffusion in unidirectional fiber structures.

constant and has an average value of 0.54 (see Tomadakis and Sotirchos, 1991a). For bulk diffusion in two- and three-directional fibrous beds, the tortuosity is larger than unity at all porosities, approaching unity at the limit of dilute beds. Shown in Figures 10 and 11 are also variational bounds presented by Tsai and Strieder (1986) for bulk diffusion in three-directional beds and perpendicularly to the fibers of two-directional structures:

$$\eta^b_{3-d} \geq 1 - \frac{2}{3}\ln\epsilon; \quad \eta^b_{y,2-d} \geq 1 - \ln\epsilon \qquad (11a,b)$$

Comparison of these bounds with our bulk tortuosity results showed that they provide very good approximations to the actual tortuosities for $\epsilon > 0.6$ and $\epsilon > 0.7$, respectively.

The bulk tortuosities for diffusion perpendicularly to unidirectional fibers were in very good agreement for porosities higher than about 70% with a lower bound proposed by Milton (1981). Milton obtained expressions for upper and lower bounds on various transport properties of fiber reinforced materials. In terms of the bulk tortuosity of a structure of impervious to diffusion fibers, Milton's expressions have the form:

$$\epsilon + \frac{2(1-\epsilon)}{\zeta} \leq \eta^b_{xy,1-d} \leq \infty \qquad (12)$$

This result is valid for all directionalities, provided that the material is statistically isotropic in the transverse plane. Parameter ζ is a characteristic of the structure and must be calculated from the three-point correlation function (Milton, 1981). Torquato and Beasley (1986) expressed ζ in the form of a multidimensional integral involving lower-order n-point probability functions and estimated its value for freely overlapping, unidirectional fiber structures of various porosities. Joslin and Stell (1986a) calculated independently the same values for ζ. They further examined the effect of fiber diameter polydispersity on ζ and found it to be insignificant (Joslin and Stell, 1986b). Smith and Torquato (1989) obtained the values of ζ for unidirectional fibers of varying extent of overlapping, through Monte Carlo measurements of the n-point probability functions that define ζ. The ζ values given in the above studies were used in Eq. 12 to construct the curve shown in Figure 13.

Figure 11 shows that the numerically computed bulk tortuosities for two-directional structures, perpendicularly to the fibers, are in very good agreement with two experimental data points by Bateman et al. (1984) and Penman (1940). Bateman et al. measured the bulk diffusivity of *NO* through various porous substrates and expressed their results as tortuosity factors. They used track-etched polycarbonate substrates having uniform cylindrical pores (for which $\eta^b = 1$) to validate their experimental results. The point shown in Figure 11 ($\eta^b = 1.5$) was obtained for diffusion perpendicularly to the fibers of a cellulosic filter, a two-directional fibrous structure, with porosity $\epsilon = 0.65$. Penman (1940) determined the bulk tortuosity of many porous solids, mostly sands, from steady-state diffusion experiments using carbon disulfide and acetone vapor. He also studied a steel wool sample of 93% porosity, for which he obtained $\eta^b = 1.14$ perpendicularly to the fibers, and this is the result plotted in Figure 11. It must be pointed out that Currie (1960a,b) applied nonsteady-state diffusion measurements to obtain diffusivity values for a variety of porous materials, including samples of fiber glass. His data are limited to very dilute beds ($\epsilon > 0.95$) and correspond to bulk tortuosity values that are 13–16% higher than those determined in our work. It is possible that these differences are due to the several difficulties encountered in the interpretation of unsteady-state diffusion-cell data (Burghardt et al., 1988; Sotirchos, 1992).

All bulk tortuosity curves from Figures 10 to 13 are summarized in Figure 14. These results can be used for the estimation of other transport properties (such as thermal and

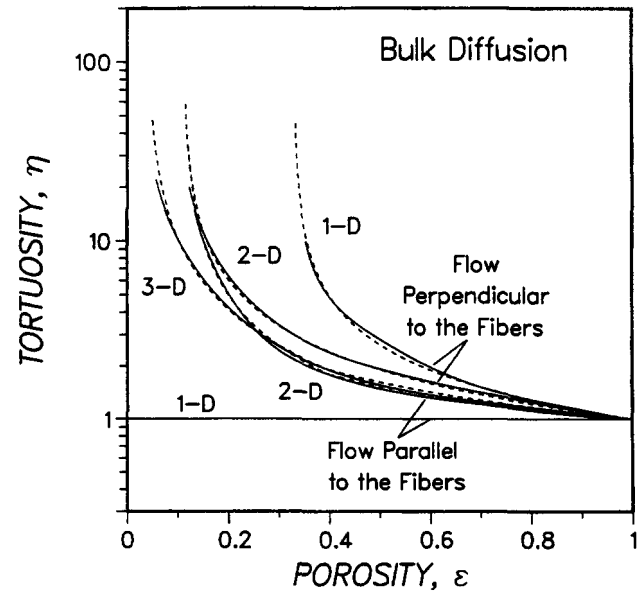

Figure 14. Tortuosities in the bulk diffusion regime for all directionalities.

The dashed curves are obtained from Eq. 13 using the parameters of Table 1.

electrical conductivity) of composite media consisting of nonconducting fibers embedded in a conducting matrix. Figure 14 shows that in two-directional structures the tortuosity factor is smaller—and the effective diffusivity is larger—parallel to the fibers. This is also true for the Knudsen diffusivity (compare Figures 11 and 12), but the difference between the results for the two directions is larger, indicating that the degree of anisotropy of two-directional structures decreases from the Knudsen to the bulk diffusion regime. This observation also holds for structures of unidirectional fibers, in agreement with the results of Figure 1, which suggest, that the ellipticity of the distribution of molecular displacements decreases as we move away from the Knudsen regime.

Like in our past studies (Tomadakis and Sotirchos, 1991a,b), an effort was made to obtain a simple one-parameter correlation for the dependence of bulk tortuosity on medium porosity. The simulation results were fitted into the equation:

$$\eta^b = \eta^b(\epsilon_0)\left(\frac{\epsilon_0-\epsilon_p}{\epsilon-\epsilon_p}\right)^{\alpha} \tag{13}$$

The percolation thresholds, ϵ_p, of all structures were calculated in our previous study (Tomadakis and Sotirchos, 1991a) and are listed in Table 1, which also gives α for each directionality and diffusion direction. These values were determined through nonlinear regression for $\epsilon_0 = 1$, and therefore, $\eta^b(\epsilon_0) = 1$ for all cases. For bulk diffusion in a three-directional structure or parallel to the fiber mat of a two-directional structure, the parameters of Table 1 do not yield satisfactory results for $\epsilon < 0.4$. For this porosity region, better results are obtained using Eq. 13 with $\epsilon_0 = 0.4$, $\alpha = 0.872$ for the 2-d structure, and $\alpha = 0.965$ for the 3-d structure, with $\eta_j^b(0.4)$ computed from Eq. 13 and Table 1. The tortuosity vs. porosity curves that are predicted by Eq. 13 are represented in Figure 14 by dashed lines. Correlation coefficients varying from 98.9 to 99.9% were obtained for all curves plotted in the figure. It should be pointed out that Eq. 13 may be viewed as a generalization of Archie's law [$\eta^b = \epsilon^{-\alpha}$, Archie (1942)] for a porous medium having finite percolation threshold.

Molecular Free Paths and Collision Frequencies

The numbers C_m of intermolecular and C_w of molecule-wall collisions are stored during the simulation, and they are used to compute the overall mean free path, $\bar{l}$, from the equation:

$$\bar{l} = \frac{sN}{C_m + C_w} \tag{14}$$

where N is the total number of random walkers and s the travel distance covered by each of them. We also keep track of where

Table 1. Parameters Used in Eq. 13

	Direction of Diffusional Flow	ϵ_p	α
1-D	Parallel to the Fibers	0	0
	Perpendicular to the Fibers	0.33	0.707
2-D	Parallel to the Fiber Planes	0.11	0.521
	Perpendicular to the Fiber Planes	0.11	0.785
3-D	All Directions	0.037	0.661

each path (step) in each molecular trajectory originates or ends (in the void space or on the solid surface), and this information is used to compute the average paths $\bar{l}_{ww}$, $\bar{l}_{mm}$, $\bar{l}_{wm}$, and $\bar{l}_{mw}$, denoting, respectively, lengths of paths from wall to wall, molecule to molecule, wall to molecule, and molecule to wall. In his study of energy deposition by neutrons in spherical cavities, Caswell (1966) refers to these paths as crossers, insiders, starters, and stoppers, respectively. Obviously, in the Knudsen diffusion regime ($Kn \to \infty$) practically all paths are crossers distributed according to the μ-randomness distribution density, while in the bulk regime nearly all paths are insiders having the distribution density of continuum diffusion free paths. Expressions for the path distribution densities in the transition regime may be derived by using a result relating the densities of μ- and l-random secants.

Let $P_\mu(d)$ be the distribution density of μ-random secants in a porous medium and $P_\lambda(\lambda)$ be the distribution density of free paths for continuum diffusion. Kingman (1965) showed that in a convex body the distribution density of l-random secants of length d is proportional to $dP_\mu(d)$. This result is valid for nonconvex domains as well—the procedure used by Coleman (1969) to prove it for convex domains can be extended to cover nonconvex bodies—and therefore, it applies to the pore space of a porous medium. It can be shown using Kingman's result (Kellerer, 1971) that the density of half l-random secants, that is, from the randomly chosen point to the boundary of the domain, is given by $\int_d^\infty P_\mu(x)dx/\bar{d}$. We mentioned during the discussion of the random walk procedure that the distribution density of lengths of paths for molecules leaving a plane after a diffuse reflection is taken the same as that of molecules reaching the plane, being given by $\int_\lambda^\infty P_\lambda(x)dx/\bar{\lambda}$. Assuming independence of the events of molecule-molecule and molecule-wall collisions, the above results may be used to show that the distribution density of paths of any type during diffusion in the transition regime in a porous medium is given by:

$$P(l) = \frac{1}{\bar{\lambda}+\bar{d}}\left[P_\mu(l)\int_l^\infty\int_{l'}^\infty P_\lambda(x)dxdl' + P_\lambda(l)\int_l^\infty\int_{l'}^\infty P_\mu(x)dxdl' + 2\int_l^\infty P_\lambda(x)dx\int_l^\infty P_\mu(x)dx\right] \tag{15}$$

Equation 15 is identical to an equation derived by Kellerer (1971) for the density of track segments lying in a convex body exposed to random tracks with distribution density $P_\lambda(\lambda)$. The three terms in the righthand side of Eq. 15 represent the contributions of crossers (l_{ww}), insiders (l_{mm}), starters and stoppers (l_{wm} and l_{mw}), respectively, the contributions of starters and stoppers being the same.

Equation 15 may be used to derive several general relations for transition regime diffusion by a random walk mechanism in porous media of arbitrary structure. By multiplying Eq. 15 by l and integrating, it is found that the mean free path during transition regime diffusion ($\bar{l}$) is related to the mean free paths during Knudsen and bulk diffusion ($\bar{d}$ and $\bar{\lambda}$) by Eq. 7:

$$\frac{1}{\bar{l}} = \frac{1}{\bar{\lambda}} + \frac{1}{\bar{d}}$$

no matter what the form of $P_\mu(d)$ and $P_\lambda(\lambda)$ is. Another

interesting result obtained from Eq. 15 is that the ratio of the number of molecule-wall to the number of molecule-molecule collisions, C_w/C_m, is equal to the Knudsen number:

$$\frac{C_w}{C_m}=\frac{\bar{\lambda}}{\bar{d}}=Kn \tag{16}$$

Combining Eq. 16 with the definition of $\bar{l}$ (Eq. 14) and Eq. 7 leads to the equally interesting results:

$$\frac{sN}{C_m}=\bar{\lambda};\quad \frac{sN}{C_w}=\bar{d} \tag{17}$$

The last two equations state that for all Knudsen numbers the average distance traveled between two intermolecular collisions is always equal to the continuum mean free path, $\bar{\lambda}$, while the corresponding average distance traveled between two molecule-wall collisions is always equal to the mean intercept length, $\bar{d}$, of the structure. Using Eq. 1c and the definition of Knudsen number, Eqs. 14 and 7 may be combined to obtain an equation that relates the total number of steps or collisions per random walker to the dimensionless travel distance and the porosity:

$$\frac{(C_w+C_m)}{N}=\frac{s}{\bar{l}}=\left(\frac{-\ln\epsilon}{2}\right)\left(1+\frac{1}{Kn}\right)(s/r) \tag{18}$$

Using this equation, the results of Figure 3 or of other similar figures can be used to determine the minimum number of collisions or steps needed to obtain accurate diffusivity measurements.

For a convex body exposed to random tracks of finite length, Kellerer (1971) used the total track length in the body and the number of terminal points of tracks to prove Eq. 7. Bosanquet based the derivation of Eq. 7 for gas self-diffusion in a cylindrical tube on the additivity of the frequencies of the two types of collisions (Pollard and Present, 1948) and used this result to postulate the harmonic average expression for transition regime diffusion in a cylindrical tube. Equation 7 is usually presented in the literature as valid for random scattering caused by collisions of two different types with exponential path densities between collisions of the same type (such as wall to wall or molecule to molecule in the case of diffusion). For this special case, the derivation of Eq. 7 is straightforward, since the overall collision probability is exponential with decay length given by Eq. 7. Such a derivation of Eq. 7 has been presented, among others, by Tokunanga (1985) for diffusion in a porous medium and by Wert and Thomson (1970) for electron scattering due to phonon collisions and impurity scattering.

Equations 7 and 16 were used to test the procedure applied for the computation of molecular trajectories in our simulations, and typical results are shown in Figures 15 and 16. The distinct data points of Figure 15 represent numerically computed values of the ratio of overall to continuum mean free path ($\bar{l}/\bar{\lambda}$) for two structures and at various Knudsen numbers, while the solid curve gives the values predicted by Eq. 7. Figure 16, on the other hand, compares the collision frequency ratios measured during trajectory computations for the same structures and Knudsen number values as in Figure 15 with the values predicted by Eq. 16 (straight line). Excellent agreement is seen to exist between the numerical results and the theoretically expected values in both figures. In their study of transition and bulk diffusion in fibrous beds, Melkote and Jensen (1992) reported values of the overall free path to continuum free path ratios measured in their simulations which deviate from that given by Eq. 7 by as much as 14%. This suggests the existence of some problems in their trajectory computations, since Eq. 7 holds rigorously for any porous medium.

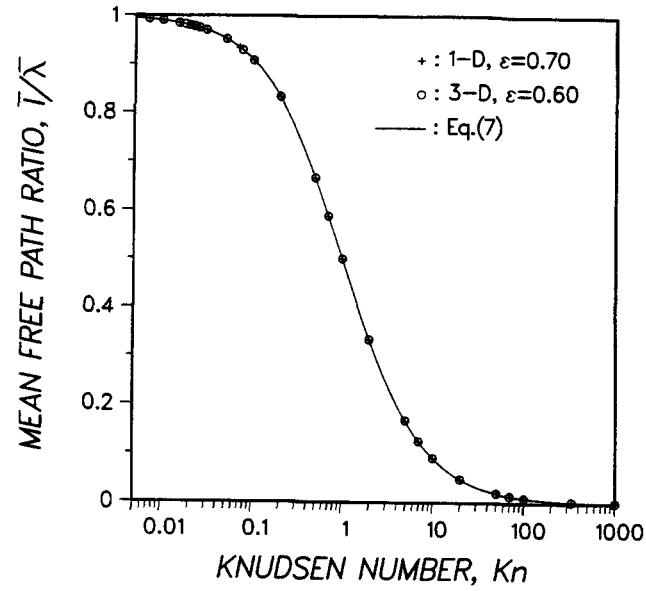

Figure 15. Variation of the overall to continuum mean free path ratio with the Knudsen number.

For structures of randomly overlapping fibers, it is possible to obtain analytical expressions for the distribution density of μ-random secants. Working along the lines of the procedure followed by Faley and Strieder (1987, 1988) to derive upper bounds on the effective Knudsen diffusivities in random fiber

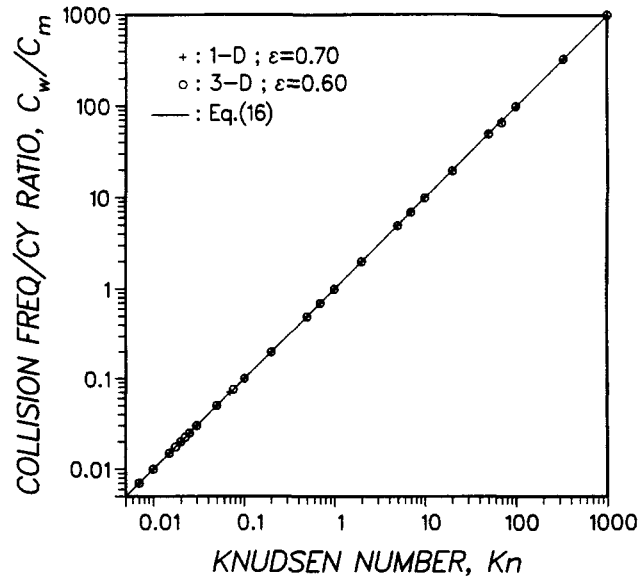

Figure 16. Variation of the ratio of molecule-wall to intermolecular collision frequencies with the Knudsen number.

beds, one can show that the following equations give the density of μ-random secants in fiber structures:

One-directional:

$$P_\mu(d) = \frac{4}{\pi\bar{d}}\int_0^{\pi/2} \exp\left(-\frac{4d}{\pi\bar{d}}\sin\beta\right)\sin^3\beta d\beta \qquad (19)$$

Two-directional:

$$P_\mu(d) = \bar{d}F^2\int_0^{\pi/2} \exp[-FdE(\sin^2\beta)]E^2(\sin^2\beta)\sin\beta d\beta; \qquad (20a)$$

$$F = \frac{8}{\pi^2\bar{d}} \qquad (20b)$$

Three-directional:

$$P_\mu(d) = \frac{1}{\bar{d}}\exp\left(-\frac{d}{\bar{d}}\right) \qquad (21)$$

$E(\sin^2\beta)$ in Eq. 20 is the complete elliptic integral of the second kind: $E(\sin^2\beta) = \int_0^{\pi/2}\sqrt{1-\sin^2\beta\cos^2\theta}d\theta$.

The path distribution densities given by Eqs. 19-21 are plotted in Figure 17, where they are compared with the numerically computed distribution densities from various simulation runs. 6.3×10^6 paths (for 11 different porosities) were used for the numerical construction of the path distribution density in three-directional structures, 6×10^5 (for one porosity value) for two-directional structures, and 5×10^6 (for 11 porosities) for one-directional structures. As in the case of Figures 15 and 16, excellent agreement is observed between theory and simulation. A comparison of the predictions of Eqs. 19-21 shows—it is difficult to discern this from Figure 17—that the path densities of the anisotropic uni- and bidirectional structures are larger than those of the isotropic tridirectional bed in the regions of small and large path values, while the opposite relation obtains in the intermediate region. The relative differences among the distribution densities for different directionalities are very small for $d/\bar{d}<5$, and for two- and three-directional fiber structures, this is true for all path values. The path density of one-directional structures deviates significantly from the densities of the other two directionalities for large path values, since paths forming small angles with unidirectional fibers have low probability to be intercepted at a small distance from the origin.

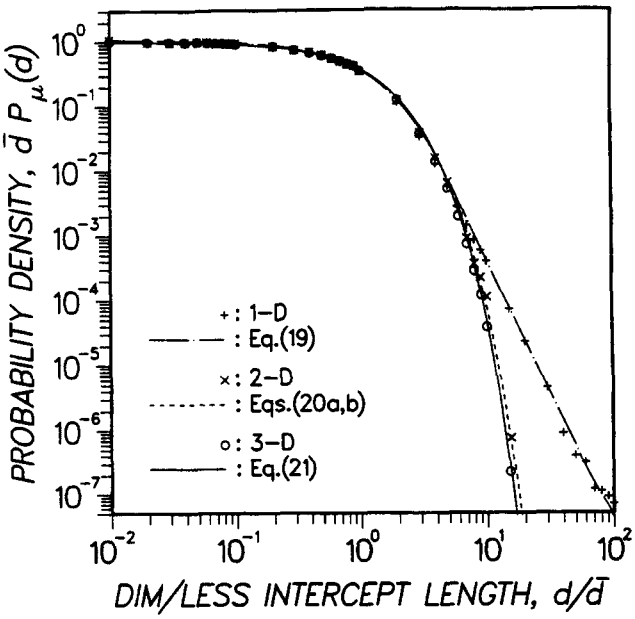

Figure 17. Distributions of intercept lengths in random fiber structures for all directionalities.

The results of Eqs. 19-21 may be introduced in Eq. 15, along with the exponential distribution of continuum diffusion free paths, to obtain results for the average lengths and relative populations of different kinds of paths during transition regime diffusion. For the case of an exponential distribution of μ-random paths (Eq. 21), Eq. 15 (the three terms in its righthand side) offers that all kinds of free paths have exponential distribution densities of the same average length ($\bar{l}$):

$$\frac{1}{\bar{l}_{ww}} = \frac{1}{\bar{l}_{mm}} = \frac{1}{\bar{l}_{wm}} = \frac{1}{\bar{l}_{mw}} = \frac{1}{\bar{l}} = \frac{1}{\bar{\lambda}} + \frac{1}{\bar{d}} \qquad (22)$$

Moreover, for the total populations of the various kinds of free paths, p_{ww}, p_{mm}, p_{wm}, and p_{mw}, the above substitutions give:

$$p_{ww}/p_{mm} = Kn^2; \quad p_{ww}/p_{wm} = Kn \qquad (23a,b)$$

Of course, we always have $p_{wm}/p_{mw} = 1$ irrespective of the forms of $P_\mu(d)$ and $P_\lambda(\lambda)$. All the above relations were found to be exactly satisfied by the results for three-directional structures. They were also valid for all practical purposes for two-directional structures, a behavior that should not surprise us considering that the secant density function of these structures does not differ significantly from the exponential form. Larger differences were observed for the highly anisotropic one-directional structures, but even in this case they rarely exceeded 5%.

Results for Biased Random Walks and Constant Free Path

It is obvious that all results presented thus far were obtained from no-memory random walks, since all directions were assumed equally probable for the molecule's path following an intermolecular collision. However, it is the direction of the two molecules' relative velocity vector after a collision that is uniformly random (Jeans, 1925; Kennard, 1938; Bird, 1976). Some persistence of velocities is always encountered: there is a moderate tendency for a succeeding path to favor the direction of the preceding one. In his analysis of self-diffusion of spherical molecules, Jeans (1925) showed that the self-diffusion coefficient is approximately given by $D^b = 0.561\bar{\lambda}\bar{v}$ when persistence of velocities is considered. He further showed that accounting for the different mean free paths of steps of different velocities leads to $D^b = 0.590\bar{\lambda}\bar{v}$. A similar result was obtained by Chapman and Cowling (1970) [$D^b = (3\pi/16)\bar{\lambda}\bar{v} = 0.589\bar{\lambda}\bar{v}$], again for rigid elastic spheres, through a different procedure. As mentioned earlier during the discussion of the formulas used to define tortuosity factors, a no-memory random walk yields $D^b = (1/3)\bar{\lambda}\bar{v}$, that is, a value smaller by

almost a factor of 2 than that obtained when persistence of velocities is taken into account. Because of this difference, it is necessary that we address the question of whether the results and conclusions presented thus far are valid only for the idealized case of a no-memory random walk and are thus not applicable to real gases diffusing in fibrous beds.

To obtain an answer to this question, we computed self-diffusion coefficients for diffusion in the gas phase and in the fiber beds by introducing some arbitrary persistence of velocities bias into the random walk procedure. Specifically, we bounded the minor angle ω formed by the vectors that represent the velocities of a molecule before and after an intermolecular collision between 0 and ω_{max}. It can be shown that the dimensionless self-diffusion coefficient in the gas phase, $D^b_\omega/(\bar{\lambda}\bar{v})$, is given. In agreement with the analysis of Jeans (1925), this expression predicts that the diffusion coefficient increases as the maximum angle is decreased and movement in the general direction followed by the molecule before collision is favored. Introduction in Eq. 8 of the bulk and transition regime diffusivities for each value of ω_{max} and of the Knudsen diffusivity—obviously, the Knudsen diffusivity is not influenced by the direction of the molecules after an intermolecular collision—led to the same conclusion as in the case of unbiased random walks. That is, Eq. 8 was again obeyed by all directional diffusivities with the exception of that parallel to unidirectional fibers.

The bulk tortuosities that are extracted from the bulk effective diffusivities using Eq. 3 and the D^b_ω self-diffusion coefficients as reference values (D_p) were identical to those obtained for unbiased random walks for all ω_{max} values. Moreover, when the D^b_ω self-diffusion coefficients were used in Eq. 4 instead of $D^b = 1/3\bar{\lambda}\bar{v}$ to find the reference diffusivity D_p, the estimated tortuosity factors from Eq. 3b were found to obey Eq. 9 with the definition of Knudsen number now generalized to $Kn = D^b_\omega/D^K$ ($=\bar{\lambda}/\bar{d}$ for an unbiased random walk, that is, $\omega_{max} = 180°$). For this definition of Kn, the diffusivities parallel to the fibers of a one-directional structure and the corresponding tortuosities satisfied the same relationships as those for unbiased walks, namely, Eqs. 10a and 10b, for the same value of γ. Even though they cannot be interpreted as a proof, the above results offer a strong indication that the bulk tortuosities extracted from unbiased random walk simulations (Figures 6–8 and 10–14) and the conclusions on the validity of the Bosanquet relationship will be valid even when a more realistic diffusion scheme is considered for the gas phase. It must be pointed out that the various results presented earlier on collision frequencies and free paths during unbiased random walks were found to be valid for biased random walks also.

From the analysis of random walks of constant step (for example, see Kennard, 1938), it is found that the mean-square displacement of a random walker moving with constant step $\bar{\lambda}$ is, for the same total travel distance, half of that of random walkers moving with an exponential distribution of steps of mean $\bar{\lambda}$. It follows from Eq. 2 that to obtain the correct self-diffusion coefficient of a gas from a random walk of constant step, one must employ steps equal to $2\bar{\lambda}$, with $\bar{\lambda}$ being the mean free path for an exponential distribution. The effects of using constant free path on the estimated effective diffusivities of fibrous beds in the transition and bulk diffusion regime were investigated in detail by carrying out simulation runs for various porosity and Knudsen number values. It was found that setting the path between intermolecular collisions equal to $2\bar{\lambda}$ yields the same diffusivity values as an exponential distribution of paths in the bulk diffusion regime, but it fails to do so in the transition regime. In general, the transition regime diffusivities for $P_\lambda(\lambda) = \delta(\lambda - 2\bar{\lambda})$ were larger than those for $P_\lambda(\lambda) = \exp(-\lambda/\bar{\lambda})/\bar{\lambda}$. This is most probably due to the fact that the ratio of the number of molecule-wall to that of intermolecular collisions for $2\bar{\lambda}$ constant path is two times larger than that for an exponential distribution of mean $\bar{\lambda}$ (see Eq. 16). The collision frequencies and average free paths that we computed from constant path simulations satisfied exactly the various general relationships that we derived earlier.

Summary and Conclusions

The problem of mass transport of gases by diffusion in structures of freely overlapping fibers of various orientation distributions has been investigated in detail. Fibrous beds consisting of unidirectional fibers, fibers randomly distributed parallel to a plane (bidirectional), or fibers oriented randomly in all directions (tridirectional) were considered. Effective diffusion coefficients were calculated using a simulation method based on the computation of the mean-square displacement of random walkers (molecules) moving in the pore space of the fibrous beds. A finite cell was employed in the simulations, but results representative of the infinite porous medium were obtained by imposing appropriate boundary conditions on the faces of the finite sample. The results from the molecular trajectory computations were used not only for the computation of the mean-square displacement but also for the determination of the frequencies of intermolecular and molecule-wall collisions and of the distribution densities of paths between collisions of the same or different type. These results were used to validate the simulation algorithm.

The transition diffusion regime was found to extend over the Knudsen number range of approximately 0.02 to 50. The effective diffusivities and, hence, tortuosities in all diffusion regimes were found to depend strongly on the directionality of the fiber structures at low and intermediate values of the porosity. The tortuosity factor diverged to infinity at the percolation threshold of each fiber bed, that is, at the porosity level below which the pore space of the medium exists in the form of finite disconnected regions. In the upper part of the porosity range (typically $\epsilon > 70\%$), the computed values of bulk tortuosity were in good agreement with lower bounds of the literature (Milton, 1981; Tsai and Strieder, 1986). For $\epsilon \to 1$, as expected, the effective diffusivity in the bulk diffusion regime approached the analytically predicted value of the self-diffusion coefficient of the gas in the absence of the porous medium. For all directionalities, the tortuosity factor increased from the bulk to the Knudsen diffusion regime. This was also observed for the relative difference between the directional diffusivities (along the principal axes of diffusion) of the unidirectional and bidirectional anisotropic structures.

One of the most interesting findings of our study was that the effective diffusivity in the transition regime can be satisfactorily approximated by the harmonic mean of the corresponding bulk and Knudsen effective diffusivities (the well-known Bosanquet approximation), except parallel to unidirectional fibers. This conclusion, as well as all other results obtained in our study, was found to be valid even when some

arbitrary persistence of velocities bias was introduced into the random walk scheme used to compute effective diffusivities. A similar conclusion on the validity of the Bosanquet approximation in the more general context of multicomponent diffusion and convection was reached by Sotirchos (1989) for pore structures consisting of networks of cylindrical capillaries. Specifically, it was found that the three-parameter dusty-gas model—which employs the bulk tortuosity, Knudsen tortuosity, and permeability of the porous medium as parameters and reduces to the Bosanquet approximation for single species diffusion (self-diffusion or tracer diffusion) under isobaric conditions—yields almost identical results to those obtained when the dusty-gas model flux relation written for a cylindrical pore is averaged over the pore-size distribution. Therefore, although they were obtained from self-diffusion simulations, the bulk and Knudsen tortuosity values in this study are applicable to the general problem of multicomponent diffusion, provided that a flux model that uses bulk and Knudsen tortuosities (scalars or tensors), like the dusty-gas model, is used to describe the diffusion process.

Acknowledgment

Acknowledgment is made to the Donors of the Petroleum Research Fund administered by the American Chemical Society for support of this research. We also thank the Pittsburgh Supercomputing Center for providing supercomputer time for the computations reported here.

Notation

a = side of the cubic unit cell, m
$\bar{d}$ = mean intercept length ($\bar{d}=4\epsilon/S$), m
D = diffusivity, m^2/s
D_e = effective diffusivity, m^2/s
Kn = Knudsen number, $Kn=\bar{\lambda}/\bar{d}$
$\bar{l}$ = overall mean free path, m
r = fiber radius, m
s = travel distance, m
S = internal surface area, m^2/m^3
$\bar{v}$ = mean thermal speed of the molecules, m/s

Greek letters

α = parameter in Eq. 13
ϵ = porosity
η = tortuosity factor
$\bar{\lambda}$ = continuum mean free path, m
$\langle\xi^2\rangle$ = mean square displacement, m^2
τ = travel time, s

Subscripts

j, x, y, z = direction of diffusional flow

Superscripts

b = bulk diffusion regime
K = Knudsen diffusion regime

Literature Cited

Archie, G. E., "Electrical Resistivity Log as an Aid in Determining Some Reservoir Characteristics," *Trans. Amer. Inst. Min. Met. Eng.*, **146**, 54 (1942).

Bateman, B. R., J. D. Way, and K. M. Larson, "An Apparatus for the Measurement of Gas Fluxes through Immobilized Liquid Membranes," *Sep. Sci. Tech.*, **19**, 21 (1984).

Bird, G. A., *Molecular Gas Dynamics*, Clarendon, Oxford (1976).

Brown, G. W., "Monte Carlo Methods," *Modern Mathematics for the Engineer*, E. F. Beckenbach, ed., McGraw Hill, New York (1956).

Burganos, V. N., and S. V. Sotirchos, "Knudsen Diffusion in Parallel, Multidimensional or Randomly Oriented Capillary Structures," *Chem. Eng. Sci.*, **44**, 2451 (1989).

Burghardt, A., J. Rogut, and J. Gotkowska, "Diffusion Coefficients in Bidisperse Porous Structures," *Chem. Eng. Sci.*, **43**, 2463 (1988).

Carman, P. C., *Flow of Gases through Porous Media*, Butterworths Scientific Publications, London (1956).

Caswell, R. S., "Deposition of Energy by Neutrons in Spherical Cavities," *Rad. Res.*, **27**, 92 (1966).

Chandrasekhar, S., "Stochastic Problems in Physics and Astronomy," *Rev. Mod. Phys.*, **15**, 1 (1943).

Chapman, S., and T. G. Cowling, *The Mathematical Theory of Non-Uniform Gases*, Cambridge Univ. Press, London and New York (1970).

Coleman, R., "Random Paths through Convex Bodies," *J. Appl. Prob.*, **6**, 430 (1969).

Currie, J. A., "Gaseous Diffusion in Porous Media: 1. A Non-steady State Method," *Brit. J. Appl. Phys.*, **11**, 314 (1960a).

Currie, J. A., "Gaseous Diffusion in Porous Media: 2. Dry Granular Materials," *Brit. J. Appl. Phys.*, **11**, 318 (1960b).

Einstein, A., *Investigations on the Theory of the Brownian Movement*, Dover, New York (1926).

Evans, R. B., and G. M. Watson, "Gaseous Diffusion in Porous Media at Uniform Pressure," *J. Chem. Phys.*, **35**, 2076 (1961).

Faley, T. L., and W. Strieder, "Knudsen Flow through a Random Bed of Unidirectional Fibers," *J. Appl. Phys.*, **62**, 4394 (1987).

Faley, T. L., and W. Strieder, "The Effect of Random Fiber Orientation on Knudsen Permeability," *J. Chem. Phys.*, **89**, 6936 (1988).

Goodman, F. O., and H. Y. Wachman, *Dynamics of Gas-Surface Scattering*, Academic Press, New York (1976).

Ho, F. G., and W. Strieder, "Asymptotic Expansion of the Porous Medium Effective Diffusivity Coefficient in the Knudsen Number," *J. Chem. Phys.*, **70**, 5635 (1979).

Ho, F. G., and W. Strieder, "Numerical Evaluation of the Porous Medium Effective Diffusivity between the Knudsen and Continuum Limits," *J. Chem. Phys.*, **73**, 6296 (1980).

Jeans, J. H., *The Dynamical Theory of Gases*, Cambridge, London (1925).

Joslin, C. G., and G. Stell, "Bounds on the Properties of Fiber-Reinforced Composites," *J. Appl. Phys.*, **60**, 1607 (1986a).

Joslin, C. G., and G. Stell, "Effective Properties of Fiber-Reinforced Composites: Effects of Polydispersity in Fiber Diameter," *J. Appl. Phys.*, **60**, 1611 (1986b).

Kellerer, A. M., "Considerations on the Random Traversal of Convex Bodies and Solutions for General Cylinders," *Rad. Res.*, **47**, 359 (1971).

Kennard, E. H., *Kinetic Theory of Gases*, McGraw-Hill, New York (1938).

Kingman, J. F. C., "Mean Free Paths in a Convex Reflecting Region," *J. Appl. Prob.*, **2**, 162 (1965).

Koch, D. L., and J. F. Brady, "The Effective Diffusivity of Fibrous Media," *AIChE J.*, **32**, 575 (1986).

Loeb, L. B., *The Kinetic Theory of Gases*, McGraw Hill, New York (1934).

Melkote, R. R., and K. F. Jensen, "Gas Diffusion in Random Fiber Substrates," *AIChE J.*, **35**, 1942 (1989).

Melkote, R. R., and K. F. Jensen, "Computation of Transition and Molecular Diffusivities in Fibrous Media," *AIChE J.*, **38**, 56 (1992).

Milton, G. W., "Bounds on the Transport and Optical Properties of a Two-Component Composite Material," *J. Appl. Phys.*, **52**, 5294 (1981).

Penman, H. L., "Gas and Vapor Movements in the Soil: I. The Diffusion of Vapors Through Porous Solids," *J. Agri. Sci.*, **30**, 437 (1940).

Perrins, W. T., D. R. McKenzie, and R. C. McPhedran, "Transport Properties of Regular Arrays of Cylinders," *Proc. R. Soc. Lond. A*, **369**, 207 (1979).

Pollard, W. G., and R. D. Present, "On Gaseous Self-Diffusion in Long Capillary Tubes," *Phys. Rev.*, **73**, 762 (1948).

Rahman, A., "Correlations in the Motion of Atoms in Liquid Argon," *Phys. Rev.*, **136**, A405 (1964).

Rothfeld, L. B., "Gaseous Counterdiffusion in Catalyst Pellets," *AIChE J.*, **9**, 19 (1963).
Schwartz, L. M., and J. R. Banavar, "Transport Properties of Disordered Continuum Systems," *Phys. Rev. B*, **39**, 11965 (1989).
Siegel, R. A., and R. Langer, "A New Monte Carlo Approach to Diffusion in Constricted Porous Geometries," *J. Col. Inter. Sci.*, **109**, 426 (1986).
Smith, P. A., and S. Torquato, "Computer Simulation Results for Bounds on the Effective Conductivity of Composite Media," *J. Appl. Phys.*, **65**, 893 (1989).
Sotirchos, S. V., "Multicomponent Diffusion and Convection in Capillary Structures," *AIChE J.*, **35**, 1953 (1989).
Sotirchos, S. V., "Dynamic Modeling of Chemical Vapor Infiltration," *AIChE J.*, **37**, 1365 (1991).
Sotirchos, S. V., "Steady-State vs. Transient Measurements of Effective Diffusivities in Porous Solids Using the Diffusion-Cell Method," *Chem. Eng. Sci.*, 1187 (1992).
Spiegler, K. S., "Diffusion of Gases Across Porous Media," *Ind. Eng. Chem. Fundam.*, **5**, 529 (1966).
Tassopoulos, M., and D. E. Rosner, "Simulation of Vapor Diffusion in Anisotropic Particulate Deposits," *Chem. Eng. Sci.*, **47**, 421 (1992).
Tokunanga, T. K., "Porous Media Gas Diffusivity from a Free Path Distribution Model," *J. Chem. Phys.*, **82**, 5298 (1985).
Tomadakis, M. M., "Transport Properties of Porous Media of Fibrous or Capillary Structure," PhD Thesis, University of Rochester, Rochester (1993).
Tomadakis, M. M., and S. V. Sotirchos, "Effective Knudsen Diffusivities in Structures of Randomly Overlapping Fibers," *AIChE J.*, **37**, 74 (1991a).
Tomadakis, M. M., and S. V. Sotirchos,"Knudsen Diffusivities and Properties of Structures of Unidirectional Fibers," *AIChE J.*, **37**, 1175 (1991b).
Torquato, S., and J. D. Beasley, "Effective Properties of Fiber-Reinforced Materials: I. Bounds of the Effective Thermal Conductivity of Dispersions of Fully Penetrable Cylinders," *Int. J. Eng. Sci.*, **24**, 415 (1986).
Torquato, S., and I. C. Kim, "Efficient Simulation Technique to Compute Effective Properties of Heterogeneous Media," *Appl. Phys. Lett.*, **55**, 1847 (1989).
Tsai, D. S., and W. Strieder, "Effective Conductivities of Random Fiber Beds," *Chem. Eng. Commun.*, **40**, 207 (1986).
Verlet, L., "Computer Experiments on Classical Fluids: I. Thermodynamical Properties of Lennard-Jones Molecules," *Phys. Rev.*, **159**, 98 (1967).
Wert, C. A., and R. M. Thomson, *Physics of Solids*, McGraw-Hill, New York (1970).
Wheeler, A., "Reaction Rates and Selectivity in Catalyst Pores," *Catalysis*, **2**, 105 (1955).
Zheng, L. H., and Y. C. Chiew, "Computer Simulation of Diffusion-Controlled Reactions in Dispersions of Spherical Sinks," *J. Chem. Phys.*, **90**, 322 (1989).

Manuscript received July 7, 1992, and revision received Sept. 14, 1992.